

Location of the Maximum Turbidity Zone and detection of fine-scale turbidity features in estuaries using high spatial resolution satellite (SPOT, Landsat) and airborne (CASI) data

D Doxaran and S J Lavender

*Institute of Marine Studies
University of Plymouth
Plymouth
PL4 8AA
United Kingdom*

Email: david.doxaran@plymouth.ac.uk ; s.lavender@plymouth.ac.uk

Abstract

The study concerns the quantification of suspended sediments in turbid estuarine waters from high spatial resolution remotely sensed data (SPOT-HRV, Landsat-ETM+, and CASI). It is applied to the following areas: the Gironde and the Loire estuaries (France), the Tamar estuary (UK), where suspended sediment concentrations (*SPM*) in surface waters vary from 10 to 2000 mg.l⁻¹. The methodology is essentially empirical. Based on in situ optical measurements, calibration relationships are established between the remote sensing reflectance (R_{rs}) signal and *SPM*. These relationships, obtained using reflectance ratios between near-infrared (NIR) and visible (VIS) wavebands, are relatively independent of the sediment grain-size and mineralogy, and of the illumination conditions (e.g. the cloud cover). Consequently, they can be applied to satellite and/or airborne images, even if no simultaneous in situ measurements were carried out concurrently with the satellite/plane overpass. The obtained results are explained using a bio-optical model. It relates the inherent and apparent optical properties of the considered estuarine waters. Scattering by sediments is modelled using the Mie theory. Absorption by sediments is modelled according to the existing knowledge in the domain. The modelled optical properties are validated by comparison with in situ measurements. The established calibration relationships allow an accurate estimation of concentrations, once satellite data are corrected for atmospheric effects. Resulting *SPM* maps from successive satellite images permit to observe the seasonal movements of the maximum turbidity zone (MTZ). The high spatial resolution of the satellite and CASI sensors can also be used to observe detailed resuspension phenomena and turbulent currents.

1 Introduction

In coastal waters, estuaries are complex environments where dissolved and particulate matter drained by rivers in upland basins are mixed with marine substances. As a consequence of the tidal asymmetry and the residual density circulation, a MTZ is formed where most of the suspended particles are trapped. Depending on the upland basins, these particles are mainly cohesive sediments (clays and silts) which settle and can form fluid mud layers during neap tides. The presence of a MTZ strongly affects biological processes. The main influence of turbidity is the limitation of light penetration in the water column, which is a factor controlling primary production. The understanding of fine sediment transport, notably in the high-turbidity zone, is also necessary to predict the fate of eventual pollutants and to design dredging strategies.

Spatial and/or aerial remote sensing is the most efficient tool for mapping the suspended particle concentrations and observing seasonal movements of turbidity in estuaries. This information is essential in the initialisation and validation of numerical hydro-sedimentary models (Siegel et al, 1999; Douillet et al, 2001), in order to quantify sedimentary fluxes and estimate the fluvial solid discharges to the ocean. However, the signal measured by ocean colour sensors is complicated in coastal waters because of the presence of terrestrial substances, such as coloured dissolved organic matter (CDOM) and suspended sediments in addition to phytoplankton. In estuaries, the characteristics (grain size, mineralogy) of the suspended particles vary depending on the upland basins, river discharge, tidal cycles and flocculation processes. These variations affect their optical properties. As a consequence, it is difficult to establish invariant and improved algorithms to quantify *SPM* (Bowers et al, 1998; Robinson et al, 1998; Froidefond et al, 1999; Moore et al, 1999). Calibration of remote sensing data usually requires simultaneous in situ measurements during satellite or airborne data acquisition, which involves systematic costly field experiments. Recent works in highly turbid estuarine waters have shown that simple and refined *SPM* quantification algorithms can be established using reflectance ratios between the NIR and VIS. The established calibration curves between reflectance ratios and *SPM* are relatively insensitive to the sediment characteristics, and also relatively insensitive to the illumination conditions (e.g. cloud cover) concurrent with the field measurements (Doxaran et al, 2002a; 2002b; 2003).

The first objective of this study is to present a simple method that can be used to quantify suspended sediments in turbid coastal waters from remote sensing data, without taking simultaneous field measurements. The validity and limits of calibration relationships established in three West European estuaries are discussed. The second objective is to apply the method to satellite and airborne data, previously corrected for the atmospheric effects, in order to observe the tidal and seasonal movements of the MTZ in a macrotidal estuary, the horizontal sediment transport and resuspension phenomena. The considered estuaries are the Gironde and the Loire (France), the Tamar (UK). The selected satellite sensors are SPOT-HRV and Landsat-ETM+; the used airborne sensor is CASI.

2 Methods

2.1 Theory

The radiometric measurement recorded within or at the top of the atmosphere by passive satellite sensors is the upwelling radiance L^* ($\text{W}\cdot\text{m}^{-2}\cdot\text{sr}^{-1}\cdot\text{nm}^{-1}$). L^* measurements can be converted into the commonly used reflectance signal, R^* (dimensionless) (Vermote et al, 1997):

$$R^* = \frac{\pi L^*}{\cos(\theta_s) \cdot E_s} \quad (1)$$

where θ_s is the solar zenith angle, E_s ($\text{W}\cdot\text{m}^{-2}\cdot\text{nm}^{-1}$) is the solar irradiance at the top of the atmosphere. The optical parameters presented in this paragraph depend on the wavelength (λ), but is omitted for clarity.

In the single scattering assumption, reflectance at the top of the atmosphere can be written as the sum of atmospheric and water contributions (Antoine and Morel, 1998; Moore et al, 1999):

$$R^* = R_{aer} + R_{ray} + t \cdot R_w \quad (2)$$

where R_{aer} is reflectance due to aerosols, R_{ray} is the Rayleigh reflectance due to scattering by air molecules, t is the diffuse atmospheric transmittance (dimensionless) and R_w is the water reflectance.

The purpose of the atmospheric correction is the determination of the atmospheric terms in equation 2, their subtraction from the top of atmosphere reflectance and retrieval of the water reflectance (R_w).

For oceanographic remote sensing applications, a specific water reflectance signal called remote-sensing reflectance (R_{rs} , in sr^{-1}) has been defined (Mobley, 1999):

$$R_{rs} (\text{sr}^{-1}) = \frac{L_w}{E_d} \quad (3)$$

where L_w ($\text{W.m}^{-2}.\text{sr}^{-1}.\text{nm}^{-1}$) is the water-leaving radiance and E_d ($\text{W.m}^{-2}.\text{nm}^{-1}$) is the downwelling irradiance incident on the water surface. The R_w signal retrieved from remote sensing data is equal to R_{rs} multiplied by π sr.

The R_{rs} signal can be related to the inherent optical properties of the water body (Gordon et al, 1975; Morel and Prieur, 1977), namely the absorption and backscattering coefficients (a and b_b), by taking into account some geometrical parameters resulting from the air-water surface transfer, and the bidirectional aspects (Morel and Gentili, 1993; 1996). In case of the turbid waters of the Gironde estuary, this relationship can be approximately written (Doxaran et al, 2002b):

$$R_{rs} \approx 0.524 \frac{f}{Q} \frac{b_b}{a+b_b} \quad (4)$$

where the mean value of the f coefficient is 0.33 and Q is a geometrical parameter taking into account the bi-directional aspects.

In turbid sediment-dominated waters, the contribution of phytoplankton can be neglected in a first approximation, and the total a and b_b coefficients can be written as the sum of the contributions of pure water (w), dissolved organic matter (y) and sediments (s) (Forget et al, 1999):

$$a = a_w + a_y + a_s \quad (5)$$

$$b_b = b_{bw} + b_{bs} \quad (6)$$

Both the absorption and backscattering coefficients of sediments (a_s and b_{bs}) can be modelled as functions proportional to the sediment concentration. As a consequence, the R_{rs} signal can be directly related to SPM , according to empirical or semi-empirical formulas (e.g. Doxaran et al, 2002b).

2.2 Material and methods

In order to retrieve horizontal distributions of SPM in estuaries, the following procedure was applied. Numerous shipboard R_{rs} measurements were recorded in different estuarine locations, and associated with water samples taken within surface waters. The collected data were used to find out an invariant empirical relationship between R_{rs} in SPOT-HRV, Landsat-

ETM+ and CASI bands with *SPM*. Satellite and airborne data from the estuaries were corrected for atmospheric effects, then converted into *SPM* using the established empirical relationships. The satellite images were selected at different periods of the year, in order to observe the seasonal movements of the MTZ. Regular vertical turbidity profiles were recorded in different stations within the estuaries, to explain and interpret the *SPM* maps produced from the remote sensing data.

Satellite atmospheric correction was computed using the 6S radiative transfer code (Vermote et al, 1997). The atmospheric gaseous composition was estimated by selecting appropriate predefined models in 6S (Midlatitude Summer, Midlatitude winter). The aerosol components cannot be predicted *a priori*. In situ wind direction and visibility data can provide information on aerosols (Doxaran et al, 2002b), but the common method used to estimate composition and concentration of aerosols is the black target one (Chavez, 1988). This method is based on the assumption that the incident solar light in NIR bands is totally absorbed by clear waters (i.e. water with very low suspended particle concentrations). As a consequence, the water-leaving radiance over such clear waters is zero in the NIR and the measured signal onboard the satellite is only due to the atmosphere (i.e. $R_w = 0$). Thus, the aerosol contribution in the NIR can be estimated. Then, considering two bands in the NIR, the Angstrom coefficient defined by Moore et al (1999) was calculated. This coefficient was used to determine the aerosol contribution in the remaining visible bands (Doxaran, 2003). Airborne atmospheric correction was computed using a recently developed “pixel by pixel” algorithm (Moore et al, 1999) adapted to airborne configurations (Lavender and Nagur, 2002).

For calibration of satellite and airborne data, in situ optical measurements were carried out using a field spectroradiometer (Spectron SE-590 and Trios RAMSES ARC-VIS). These sensors record a radiance signal between 380 and 950 nm in 256 channels, with an acceptance angle of 6° (field of view). The measurement procedure and determination of the R_{rs} signal have been previously described (Doxaran et al, 2002a; 2002b; 2003). To summarise, three successive above-water radiance measurements were recorded: the upwelling radiance (L_u), sensor pointing towards nadir; the downwelling radiance (L_d), sensor pointing towards a spectralon target; the sky radiance (L_s), sensor pointing towards the zenith.

Then, from the recorded hyperspectral values, the R_{rs} signal in wavebands of the selected satellite and airborne sensors was determined by taking into account their spectral sensitivity. For each optical measurement, a water sample was collected at 0.5 metre below the surface, then filtered (filters Whatman GF/F) in order to determine the *SPM* concentration.

2.3 Data

A total of 132 field measurements have been carried out in the Gironde estuary (Figure 1) between 1996 and 2001. The *SPM* range is: 10 – 2000 mg.l⁻¹ (Doxaran et al, 2003). A total of 66 similar field measurements have been carried out in the Loire estuary in 2002; the *SPM* range is: 40 – 2600 mg.l⁻¹ (Doxaran et al, 2003). A total of 50 field measurements have been carried out in the Tamar estuary in 2003, corresponding to *SPM* between 15 and 500 mg.l⁻¹. These data sets are representative of different tidal and seasonal conditions in the two estuaries. Each one of the measurements represents a calibration point between the R_{rs} signal in satellite bands and *SPM*.

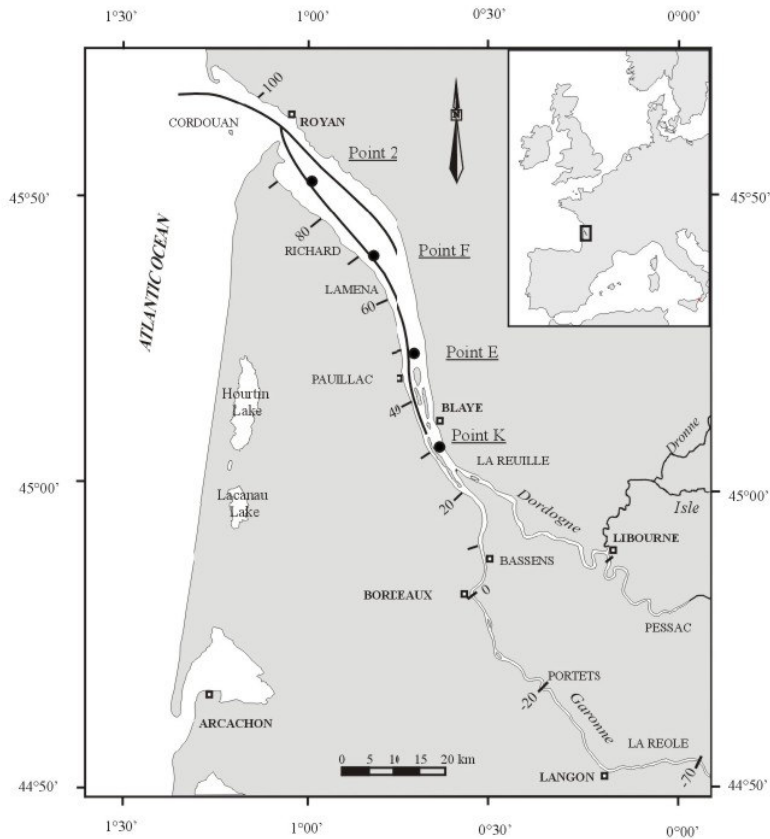


Figure 1 Map of the Gironde estuary (South-West of France). The black thick lines represent the main channels. The four black circles locate the fixed stations where most of the field measurements were carried out. Kilometre points (KP) delimit the estuary; KP 0 is Bordeaux (Garonne river) and KP 90 is the mouth.

The SPOT-HRV and Landsat-ETM+ sensors have been selected for this study, due to their spatial resolution (20 m and 30 m, respectively) that is spatially consistent with the dimensions of estuaries. The SPOT-HRV sensor has two wavebands in the visible, XS1 (500 – 590 nm) and XS2 (610 – 680 nm), and one waveband in the NIR, XS3 (790 – 890 nm) ([web site http://www.spotimage.fr/accueil/system/introsat/select/welcome.htm](http://www.spotimage.fr/accueil/system/introsat/select/welcome.htm)). The Landsat-ETM+ sensor has three bands in the visible, L1 (450 – 515 nm), L2 (525 - 605 nm) and L3 (630 – 690 nm), and two bands in the NIR, L4 (750 - 900 nm) and L5 (1550 - 1750 nm) ([web site http://landsat.gsfc.nasa.gov/guides/LANDSAT-7_dataset](http://landsat.gsfc.nasa.gov/guides/LANDSAT-7_dataset)). Seven satellite images of the Gironde estuary were considered in this study: six SPOT images recorded in 1996 and 2001; one Landsat image recorded in 2000 (see Table 1 for details). These images were selected at different periods of the year, in order to illustrate the seasonal movements of the MTZ. Airborne CASI data recorded over the Tamar estuary in 1995 are also considered in this study. CASI is a spectrophotometer that is capable of high spectral and spatial resolution. In 1995, it flown at altitudes of 3000 and 1550 m over the Tamar, with a band set of 14 wavebands designed to match up to SeaWiFS (Lavender and Nagur, 2002).

Two difficulties were encountered when applying the satellite atmospheric correction scheme. The first one was to locate black targets on the satellite images. These targets were located where the R^* signal was minimum in the NIR. Depending on the satellite images, these targets were lake waters or continental shelf waters beyond the influence of the turbid plume. On the SPOT image recorded the 17/08/2001 and covering the central and upstream parts of the estuary, these selected black targets (open ocean or lake waters) didn't appear. The 6S aerosol model was

consequently determined according to the meteorological data (wind speed and direction, horizontal visibility) available at different stations around the estuary. The second difficulty was the number of SPOT spectral bands in the NIR. Only one NIR band (XS3) was available for the sensor onboard the SPOT 1, 2 and 3 satellites. In order to calculate the Angstrom coefficient (equation 9), it was consequently assumed that the water-leaving radiance in the red band (XS2) was also zero. Such an assumption may have lead to a slight overestimation of the aerosol contribution. Concerning the Landsat data, the L4 and L5 NIR bands were selected to calculate the Angstrom coefficient.

Table 1 Details of the satellite images of the Gironde estuary. θ_v is the viewing zenith angle.

Date	Time (GMT)	Satellite	Sensor	θ_v (°)
14/07/1996	11h23'40	SPOT-3	HRV-1	+ 23.7
08/03/2000	10h40'22	LANDSAT-7	ETM+	+ 00.0
20/05/2001	11h10'23	SPOT-2	HRV-1	+ 01.2
31/05/2001	10h58'50	SPOT-2	HRV-2	- 15.4
31/05/2001	11h30'51	SPOT-1	HRV-2	+ 27.5
02/07/2001	11h15'49	SPOT-1	HRV-1	+ 05.9
17/08/2001	11h31'53	SPOT-1	HRV-1	+ 30.0

3 Results

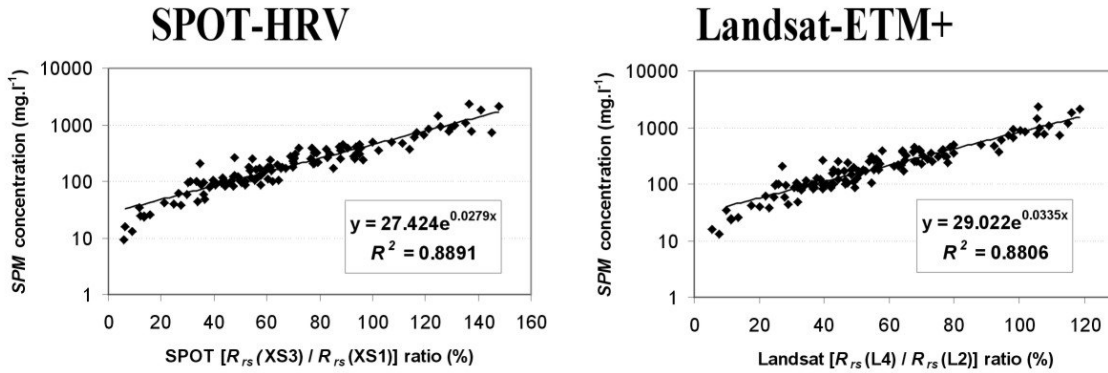
3.1 Calibration relationships

In turbid sediment-dominated waters, improved calibration relationships can be established between R_{rs} ratios and SPM . Such results were first obtained from theoretical calculations (Moore et al, 1999) or using a bio-optical model (Doxaran et al, 2002a). They were confirmed by numerous field measurements carried out in two different estuaries (Doxaran et al, 2002a; 2002b; 2003). In turbid sediment-dominated waters, R_{rs} ratios between two NIR bands or between a NIR and a visible band are highly correlated to SPM . Such R_{rs} ratios are relatively insensitive to the characteristics of the suspended sediments (Moore et al, 1999; Doxaran et al, 2003), and relatively insensitive to changing illumination conditions (notably the cloud cover) at the moment of field optical measurements (Doxaran et al, 2003).

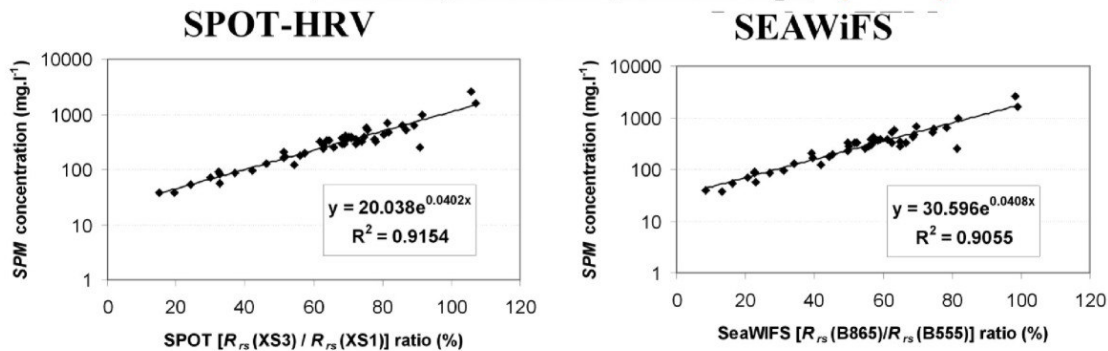
As a consequence, invariant relationships have been established between R_{rs} ratios and SPM in the Gironde estuary, from numerous field measurements carried out during a six years study (Doxaran et al, 2003). Similar relationships have been established in the Loire estuary from field measurements carried out during a three months study (Doxaran et al, 2003), then in the Tamar estuary in 2003 (Figure 2). In the Gironde estuary, the relationships were established from 18 data points in 1996, 27 in 1997, 32 in 1999, 39 in 2000 and 16 in 2001. Different conditions of tide, river flow and cloud cover were encountered during the field measurements essentially carried out in four fixed stations (Figure 1) representative of the different parts of the estuary. As a result, invariant exponential calibration curves were established between R_{rs} ratios in SPOT bands (XS3 / XS1) or Landsat bands ((L4 / L2) (Figure 2) and SPM in the range 15 – 2000 mg.l⁻¹. The R_{rs} ratios increase with increasing SPM . These calibration curves are valid at

least for the 1996 – 2001 period. They can be used to calibrate satellite data recorded during this period even if no field measurements were carried out at the moment of the satellite overpass, which was the initial objective of the study.

Selected calibration relationships : (Gironde)



Selected calibration relationships : (Loire)



First results obtained in the Tamar estuary:

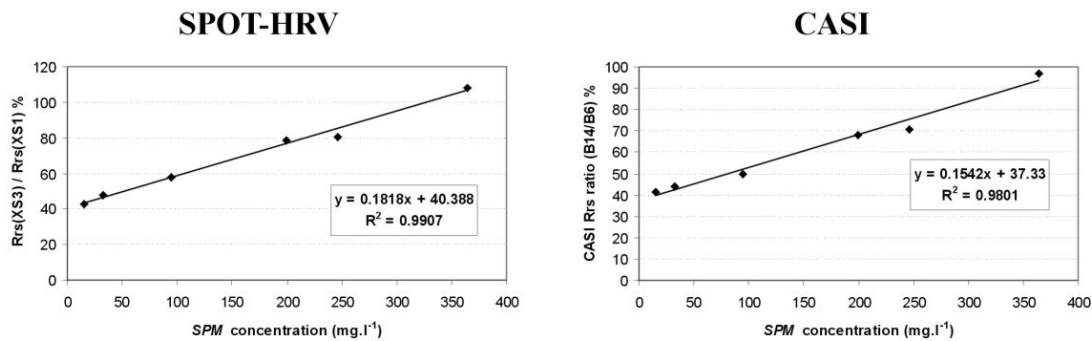


Figure 2 Selected calibration relationships between reflectance ratios and SPM for the Gironde (top), the Loire (middle) and the Tamar (bottom) estuaries.

In the Loire estuary, relationships were established from 66 data recorded in 2002 (39 in February, 11 in March and 16 in April) during flood events. Different conditions of tide and cloud cover were encountered during the field measurements carried out in the central and downstream parts of the estuary (Doxaran et al. 2003). As a result, an invariant exponential

calibration curve was established between the R_{rs} ratio in SPOT bands (XS3 / XS1) and SPM in the range 40 – 2600 mg.l^{-1} (Figure 2). Its validity, at least for the February to March 2002 period, can be used to calibrate satellite data from the estuary. The calibration curve in SPOT bands is only slightly different from the one established in the Gironde, as the characteristics of the suspended sediments are similar in the two estuaries (Doxaran et al, 2003). From our hyperspectral R_{rs} measurements, equivalent calibration relationships can be adapted to any satellite sensor, such as SeaWiFS (Figure 2). As similar calibration curves were obtained in the Gironde, Loire and Tamar estuaries (Figure 2), it tends to prove that such results may be established in most of turbid waters where SPM is higher than 10 mg.l^{-1} .

3.2 Atmospheric correction

The satellite atmospheric correction has been processed assuming that the atmosphere was homogeneous over the whole estuary. The established relationships between R^* and R_w are practically linear (Doxaran et al, 2002a). Such an assumption does not take into account the universally adopted for ocean colour sensors “pixel by pixel” correction scheme, which requires at least two wavebands in the NIR and a good knowledge of the inherent optical properties of the water body (e.g. Moore et al, 1999). However, it is interesting to note, according to these results, that the water reflectance signal was predominant compared to the atmospheric contribution. In clear oceanic waters, the water-leaving signal generally represents about 10% of the signal at the top of the atmosphere (Mobley, 1994). According to our results, for the lowest retrieved turbidity, the water-leaving signal represents at least more than 60% of the total signal measured on board the satellite. The atmospheric contribution is always higher in the NIR than in the visible, and minimum in the red part of the spectrum. Concerning the mean turbidity pixels, the atmospheric contribution strongly decreases and is typically lower than 10% of the total signal. For the maximum turbidity, the atmosphere contribution becomes practically insignificant (lower than 3%), especially in the red and NIR. These obtained results are due to the high suspended solids concentrations in water, that involves a high scattering and notably backscattering of the incident irradiance. This is contrary to clear ocean waters where absorption by pure water is usually high compared to the scattering properties of phytoplankton. As a practical consequence, and according to the obtained results, the uncertainty of the atmospheric correction only slightly affects the uncertainty of the retrieved SPM . The SPM retrieval uncertainty thus essentially depends on the calibration relationships based on R_{rs} ratios. Current works aim at confirming these results using an improved “pixel by pixel” correction algorithm (Moore et al, 1999; Lavender and Nagur, 2002).

3.3 Application: seasonal movements of the MTZ in the Gironde estuary

After applying the atmospheric correction, the calibration relationships established in the Gironde were applied to the satellite data. Horizontal distributions of turbidity within the surface waters of the estuary were established for each satellite image, locating the MTZ and observing its seasonal movements.

The first image (SPOT-HRV, 14/07/1996, 11h23) describes the situation during a low river flow period, for mean tides. It was recorded during the start of the flood in the downstream part of the estuary, corresponding to the low water slack tide in the central part and the ending ebb in the upstream part. Decreasing SPM were observed from the upstream part to the mouth (Figure 3). Two MTZ were located: one in the central part of the estuary, around the islands and a second

upstream the confluence zone of the rivers. High *SPM* concentrations were observed along the main navigation channel, along the left shore, where suspended sediments were transported downstream during the ebb tide.

The second image (Landsat-ETM+, 08/03/2000, 10h40) is representative of very different conditions: spring tides and high river flow (peak flood). It was taken around mid ebb in the central part of the estuary. High *SPM* concentrations were observed in the whole estuary (Figure 3). The lowest *SPM* concentrations were located in the rivers and in the upstream part. Resulting from successive floods, the MTZ moved into the central and downstream parts of the estuary, and was partly expelled towards the ocean during the ebb.

The third image (SPOT-HRV, 20/05/2001, 11h10) was recorded during mean tides, the last day of a six month-long high river flow period. As a consequence, the *SPM* concentrations were low in the whole estuary (Figure 3). A “residual” MTZ, after being partly expelled in the ocean, was located in the central part of the estuary. High *SPM* were also observed in front of the kilometer point (KP) 60, probably resulting from resuspension over mud banks.

The river flow rapidly decreased after the 20/05/2001. Ten days later, two satellite images (SPOT-HRV, 31/05/2001, 10h58 and 11h30, respectively) show the influence on the location of the MTZ. As a result of the decreasing river flow, it moved rapidly upstream (estimated mean velocity of 1.4 km per day), reaching the confluence zone of the Garonne and Dordogne rivers (Figure 4). High *SPM* concentrations were still observed in front of the KP 60.

The next image (SPOT-HRV, 02/07/2001, 11h16) only concerned the central and downstream parts of the estuary. It was taken for mean tides, at the beginning of the low river flow period. According to the established *SPM* map (Figure 4), the MTZ was still located in the central and upstream parts. Downstream, turbid features were observed over most of the mud and sandbanks, resulting from resuspension phenomena.

The last image (SPOT-HRV, 17/08/2001, 11h32) concerned the central and upstream parts of the estuary. It was recorded for mean tides, after a three month-long low river flow period. As a consequence, the main MTZ moved into the rivers (Figure 4), but a secondary one was also observed in the central part of the estuary, where sediments were trapped in the islands zone. Resuspension phenomena were still observed over mud banks in front of the KP 60, which finally resulted in a global 70 km-long MTZ.

To summarize, the following observations were made on the different images.

- the range of the retrieved *SPM* was always totally realistic according to the previous field turbidity measurements carried out in the estuary (e.g. [Allen et al, 1977](#); [Castaing, 1981](#); [Sottolichio et al, 2001](#)). These results indirectly validate the applied algorithm. However, a rigorous validation based on simultaneous in situ optical measurements and satellite data acquisition is needed;
- the seasonal movements of the MTZ observed or deduced from the analyzed satellite images were also in agreement with previous observations (e.g. [Allen et al, 1977](#); [Castaing, 1981](#); [Sottolichio et al, 2001](#)) and with recent observations made from turbidity profiles regularly measured at different fixed stations in 2001 ([Doxaran, 2003](#)).

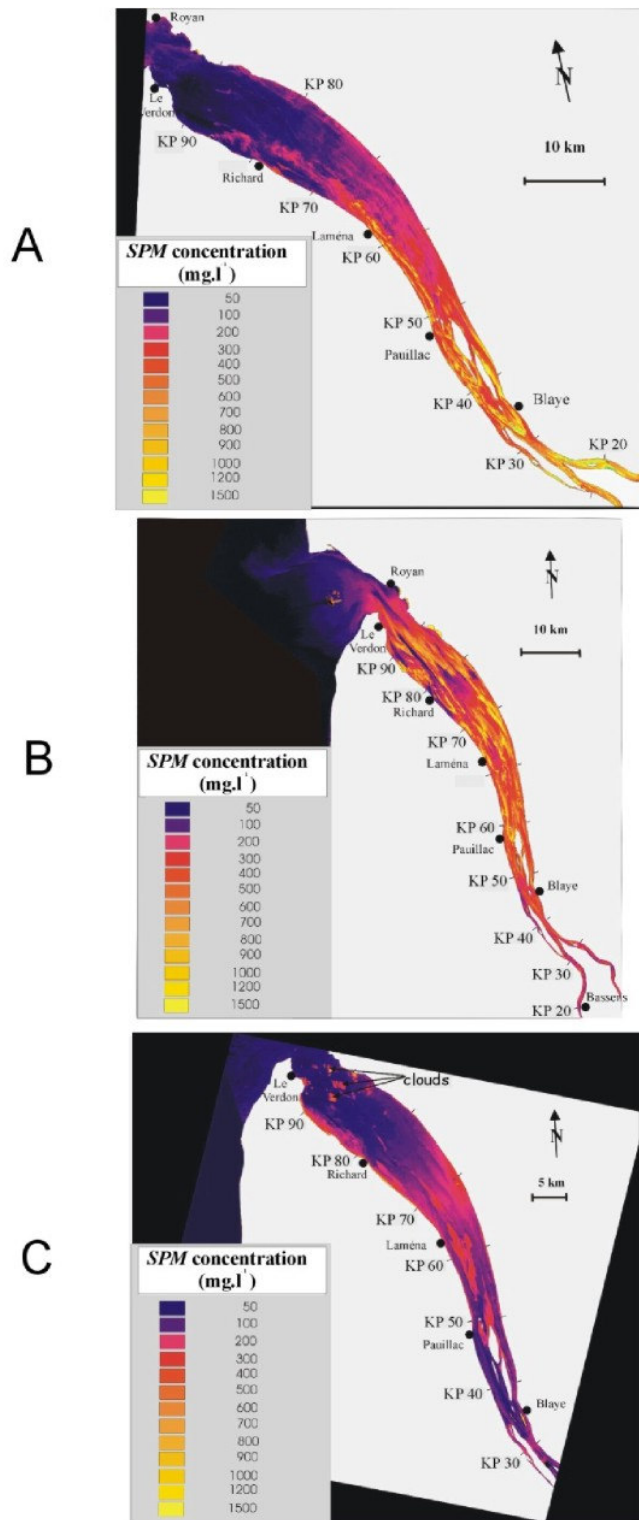


Figure 3: SPM maps established from satellite data of the Gironde estuary. A) SPOT-HRV 14/07/1996, 11h23. B) Landsat-ETM+ 08/03/2000, 10h40. C) SPOT-HRV 20/05/2001, 11h10.

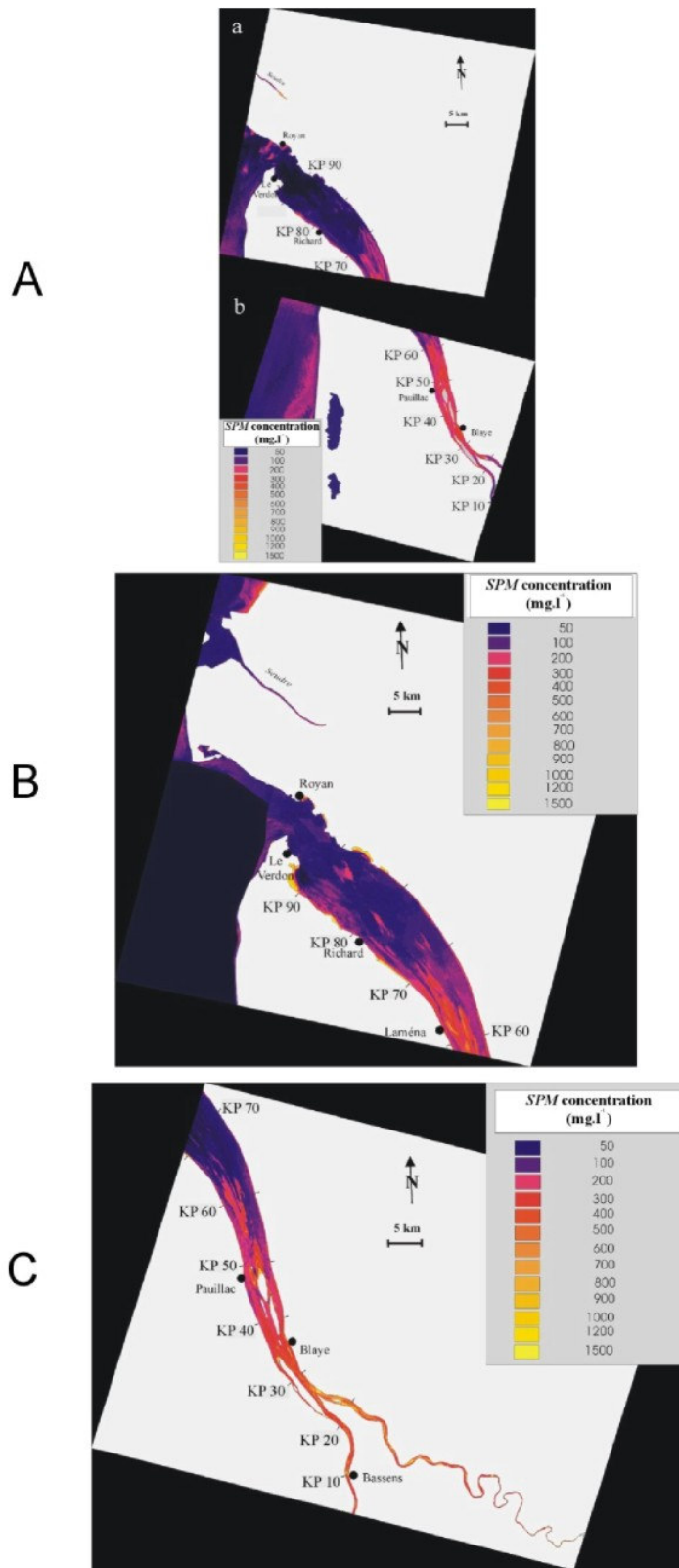


Figure 4: SPM maps established from satellite data of the Gironde estuary. A) SPOT-HRV 31/05/2001, 10h58 (a) and 11h30 (b). B) SPOT-HRV 02/07/2001, 11h16. C) SPOT-HRV 17/08/2001, 11h32.

The high spatial resolution of the SPOT-HRV and Landsat-ETM+ sensors can also be used to locate detailed resuspension phenomena, and observe turbulent flows. In fact, suspended particles within surface waters act as current markers at the moment of the image acquisition. As an example, on the SPOT image of the Gironde estuary recorded in July 1996, it is possible to observe (Figure 5):

- a turbulent flow in the upstream part, along the navigation channel. This turbulent flow occurs at the end of the ebb tide, when the mixed waters from the Garonne and Dordogne rivers enter in a narrow channel along the left shore, in front of the islands.
- parallel laminar flows in the central part, during the low water slack tide. However, results of resuspension over mud banks are still visible along the shores.
- parallel laminar flows are also present in the downstream part, notably along the main navigation channel. At the beginning of the flood, resuspension phenomena are already visible over the sandbanks. Turbid features draw the exact morphology of the banks. Complex turbid features appear near the mouth, probably resulting from settling particles transported by increasing flood currents.

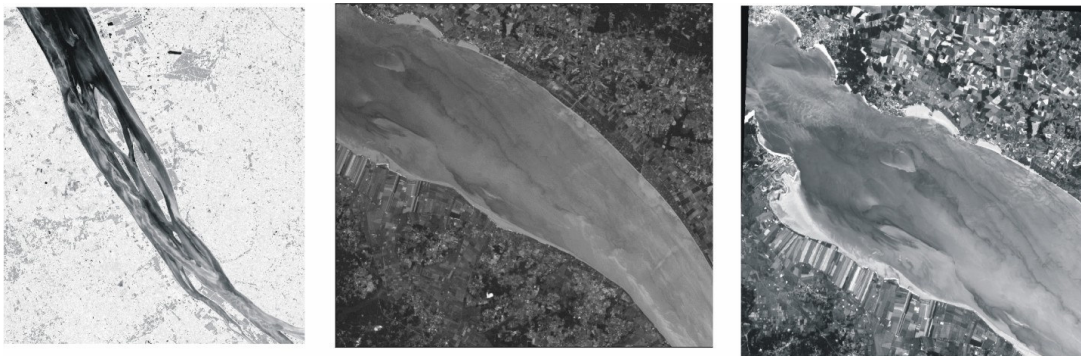


Figure 5: Turbid features observed within surface waters of the Gironde estuary on a SPOT image dated the 14/07/96, 11h23' U.T. Upstream part (left); central part (middle) and downstream part (right).

4 Conclusion

A simple and operational method was presented to quantify the suspended sediment concentrations in turbid estuarine waters using satellite or airborne imagery. Results were obtained from applying the method to a set of images from the Gironde estuary.

The method is based on calibration relationships between R_{rs} ratios (NIR / Vis) and suspended sediment concentrations. Such relationships are invariant and valid for a long-term, because R_{rs} ratios are relatively insensitive to the variations of the sediment characteristics and relatively insensitive to the illumination conditions. They provide remote sensing estimates without field measurements during the satellite or airborne overpass. They have been established for three different estuarine environments (the Gironde and the Loire, in France; the Tamar in UK) and may be extended to most of the turbid sediment-dominated coastal waters. Current research aims at reproducing the results using a theoretical reflectance model, in order to develop improved algorithms for satellite and airborne sensors. The model will determine the calibration relationship from the sediment characteristics in a studied area and according to the sensitivity of the selected optical sensor (e.g. MERIS, MODIS, CHRIS-PROBA).

Before applying the established relationships, satellite data were corrected for atmospheric affects, assuming that the atmosphere was homogeneous over the whole selected images. This simple correction scheme will be improved, using recent “pixel by pixel” corrections schemes (e.g. Moore et al, 1999). However, an important result was revealed: the reduced influence of the atmosphere on satellite data over highly scattering turbid estuarine waters. As a consequence, the *SPM* retrieval uncertainty essentially depends on the calibration relationships between the R_{rs} signal and *SPM*.

The method was applied to satellite data from the Gironde estuary. Concluding results were obtained in terms of retrieved sediment concentrations and turbidity maps. The high spatial resolution of the SPOT and Landsat sensors can be used to locate the seasonal movements of the MTZ, and gives observation of detailed turbidity features resulting from resuspension phenomena. Such information can be used to calibrate and validate numerical transport models (Siegel et al, 1999; Douillet et al, 2001). The applied method still needs to be validated with match-ups (simultaneous in situ and remote sensing measurements). The method will soon be applied to airborne imagery (e.g. CASI), which will facilitate its validation.

5 Acknowledgements

This study was financed by the Conseil general d'Aquitaine (France), and partly supported through a European Community Marie Curie fellowship (NCR 70037, Fifth Framework Programme).

6 References

- ALLEN G P, SAUZAY, G., CASTAING, P. and JOUANNEAU, J.M., 1977, Sediment transport processes in the Gironde estuary. In *Estuarine processes*, edited by M Wilet (Academic Press, New York), p. 63-81.
- ANTOINE D and MOREL, A., 1998, Relative importance of multiple scattering by air molecules and aerosols in forming the atmospheric path radiance in the visible and near-infrared parts of the spectrum. *Applied Optics*, **37**, 2245-2259.
- BOWERS D G, BOUDJELAS, S. and HARKER, G.E.L., 1998, The distribution of fine sediments in the surface waters of the Irish Sea and its relation to tidal stirring. *International Journal of Remote Sensing*, **19**, 2789-2805.
- CASTAING P, 1981, Le transfert à l'océan des suspensions estuariennes. Cas de la Gironde. *Thèse d'Etat, Université Bordeaux I*, n° 701, 530 p.
- CHAVEZ, P.S., Jr., (1988), An improved dark-object subtraction technique for atmospheric scattering correction of multispectral data. *Remote sensing of environment*, **24**, 459-479.
- DOXARAN D, 2002, Teledetection and modelisation des flux sédimentaires dans l'estuaire de la Gironde. *These de 3eme Cycle, Université Bordeaux I*, n° 2612, 284 p.
- DOXARAN D, FROIDEFOND, J.M., LAVENDER, S.J. and CASTAING, P., 2002a, Spectral signature of highly turbid waters. Application with SPOT data to quantify suspended particulate matter concentrations. *Remote Sensing of Environment*, **81**, 149-161.
- DOXARAN D, FROIDEFOND, J.M. and CASTAING, P., 2002b, A reflectance band ratio used to estimate suspended matter concentrations in sediment-dominated coastal waters. *International Journal of Remote Sensing*, **23**, 5079-5085.
- DOXARAN D, FROIDEFOND, J.M. and CASTAING, P., 2003, Remote sensing reflectance of turbid sediment-dominated waters. Reduction of sediment type variations and changing illumination conditions effects using reflectance ratios. *Applied Optics*, **42**, 2623-2634.
- DOUILLET P, OUILLOIN, S. and CORDIER, E., 2001, A numerical model for fine suspended sediment transport in the south-west lagoon of New-Caledonia, *Corals Reefs*, **20**, 361-

- FORGET P, Ouillon, S., LAHET, F. and BROCHE, P., 1999, Inversion of reflectance spectra of non-chlorophyllous turbid coastal waters. *Remote Sensing of Environment*, **68**, 264-272.
- FROIDEFOND J M, CASTAING, P. and PRUD'HOMME, R., 1999, Monitoring suspended particulate matter fluxes and patterns with the AVHRR/NOAA-11 satellite: application to the Bay of Biscay. *Deep Sea Research II*, **46**, 2029–2055.
- GORDON H R, BROWN, O.B. and JACOBS, M.M., 1975, Computed relation between the inherent and apparent optical properties of a flat homogeneous ocean. *Applied Optics*, **14**, 417 - 427.
- MOBLEY C D, 1994. *Light and water*. (Academic Press).
- MOBLEY C D, 1999, Estimation of the remote-sensing reflectance from above-surface measurements. *Applied Optics*, **38**, 7442 - 7455.
- MOORE G F, AIKEN, J. and LAVENDER, S.J., 1999, The atmospheric correction of water colour and the quantitative retrieval of suspended particulate matter in Case II waters: application to MERIS. *International Journal of Remote Sensing*, **20**, 1713-1733.
- MOREL A and PRIEUR, L., 1977, Analysis of variations in ocean color. *Limnology and Oceanography*, **22**, 709 - 722.
- MOREL A and GENTILI, B., 1993, Diffuse reflectance of oceanic waters. II. Bidirectional aspects. *Applied Optics*, **32**, 6864–6879.
- MOREL A and GENTILI, B., 1996, Diffuse reflectance of oceanic waters. III. Implication of bidirectionality for the remote-sensing problem . *Applied Optics*, **35**, 4850-4861.
- ROBINSON M C, MORRIS, K.P. and DYER, K.R., 1998, Deriving fluxes of suspended particulate matter in the Humber estuary, UK, using airborne remote sensing. *Marine Pollution Bulletin*, **37**, 155–163.
- SIEGEL H, GERTH, M. and MUTZKE, A., 1999, Dynamics of the Oder river plume in the Southern Baltic Sea: satellite data and numerical modelling. *Continental Shelf Research*, **19**, 1143-1159.
- SOTTOLICHIO A, LE HIR, P. and CASTAING, P., 2001, Modelling mechanisms for the turbidity maximum stability in the Gironde estuary, France. In: *Coastal and estuarine fine sediment transport processes*, edited by W H McAnally and A J Mehta (Elsevier, Amsterdam), p. 373 – 385.
- VERMOTE E F, TANRE, D., DEUZE, J.L., HERMAN, M. and MORCRETTE, J.J., 1997, Second Simulation of the Satellite Signal in the Solar Spectrum: An Overview. *IEEE Transactions in Geosciences and Remote Sensing*, **35**, 675-686.